CHEMNANOMAT

CHEMISTRY OF NANOMATERIALS FOR ENERGY, BIOLOGY AND MORE

www.chemnanomat.org

## Accepted Article

**Title:** 6-triphenylphosphinehexanoic acid conjugated near-infrared persistent luminescence nanoprobe for autofluorescence-free targeted imaging of mitochondria in cancer cells

**Authors:** Yu-Bin Su, Xu Zhao, Li-Jian Chen, Hai-Long Qian, and Xiu-Ping Yan



**To be cited as:** *ChemNanoMat* 10.1002/cnma.201900697

**Link to VoR:** http://dx.doi.org/10.1002/cnma.201900697

A Journal of

ACES Asian Chemical Editorial Society

A sister journal of **Chemistry – An Asian Journal** and **Asian Journal of Organic Chemistry**

WILEY-VCH

WILEY-VCH

DOI: 10.1002/ xxxxxxxxx)

Article type: Full Paper

# 6-triphenylphosphinehexanoic acid conjugated near-infrared persistent luminescence nanoprobe for autofluorescence-free targeted imaging of mitochondria in cancer cells

*Yu-Bin Su, Xu Zhao, Li-Jian Chen, Hai-Long Qian, and Xiu-Ping Yan**

Y.-B. Su, Dr. X. Zhao, Dr. L.-J. Chen, Dr. H.-L. Qian, Prof. X.-P. Yan
State Key Laboratory of Food Science and Technology, Jiangnan University, Wuxi 214122, China
International Joint Laboratory on Food Safety, Jiangnan University, Wuxi 214122, China
Institute of Analytical Food Safety, School of Food Science and Technology, Jiangnan University, Wuxi 214122, China
E-mail: xpyan@jiangnan.edu.cn

WILEY-VCH

**Abstract**

Mitochondrion, as the energy provider for cells, plays a key role in cell physiological processes. Mitochondrion-targeted imaging is of great significance for understanding the physiological functions and pathology involved in various diseases. Herein, we report the fabrication of 6-triphenylphosphinehexanoic acid (TPP) conjugated near-infrared persistent luminescence nanoparticles (PLNP) (PLNP-TPP) for mitochondria-targeted imaging in cancer cells. The PLNP was prepared by doping Cr(III) into gallogermanate through a hydrothermal method. The as-prepared PLNP showed small size, monodispersity, excellent near-infrared (NIR) luminescence and visible light renewable NIR luminescence. The grafted TPP facilitated the transportation of PLNP-TPP across the mitochondrial membrane and enabled staining of the mitochondrial region in live cancer cells. This work provides a promising strategy for fabricating PLNP nanoprobes to realize mitochondrial-targeting bioimaging.

**Keywords**: persistent luminescence; nanoprobe; mitochondria; cancer cells; bioimaging

## 1. Introduction

In most eukaryotic cells, subcellular organelle plays a critical role in various cell physiological and pathological processes, such as cell proliferation, protein synthesis, organism metabolism and cell apoptosis.[1-5] As one of the vital organelles, mitochondria act as the energy provider for cells.[6] The dysfunction of mitochondria relates to various aberrant regulations and multiple diseases including cardiovascular, blindness and neurodegenerative diseases as well as cancers.[7-9] In this sense, the targeting and imaging of mitochondria can give important implications for understanding physiological functions and pathology involved in various diseases.

To meet the unmet needs for the purpose mentioned above, a diverse array of mitochondria-targeting luminescent probes have been developed, including organic dyes,[10] fluorescent peptide,[11] fluorescent-label DNA,[12] semiconductor nanocrystals,[13] and polymer fluorescent platforms.[14-17] Despite these luminescent probes have been successfully applied for the mitochondria imaging depending on their own specific advantages, some drawbacks could not be neglected, especially the inevitable tissue autofluorescence interference. Moreover, organic dyes usually suffer from photobleaching. Polymer fluorescent platforms can be flexibly designed for optimal optical properties, but usually require complicated synthesis process.[16,17] Thus, it is still an unprecedented challenge to develop photostable probes for autofluorescence free targeted imaging of mitochondria with high specificity and biocompatibility.

Persistent luminescence nanoparticles (PLNP), which can slowly emit luminescence for hours or days even after the cessation of ultraviolet excitation, have attracted considerable attention due to their unique optical property and potential applications in optoelectronic devices, night illumination, military forces and biology.[18-20] In particular, recently developed near-infrared (NIR)-emitting PLNPs are ideal candidate phosphors for bioimaging and therapy owing to their biotissue-penetrable NIR persistent luminescence as well as efficient

avoidance of tissue autofluorescence interference.[21,22] NIR-emitting PLNPs with long afterglow time have been applied for long-term in vivo targeted tumor imaging and real-time monitoring of living mice,[23,24] especially, Cr(III)-doped zinc gallate and gallogermanate nanoparticles, which can be excited repeatedly in vivo by 808 nm or red light-emitting diode (LED) light.[19,25,26] However, to the best of our knowledge, PLNP has not been applied to subcellular structures so far.

Herein, we report 6-triphenylphosphinehexanoic acid (TPP) conjugated NIR-emitting PLNP (PLNP-TPP) for autofluorescence-free targeted imaging of mitochondria in cancer cells. Cr(III)-doped gallogermanate nanoparticles with visible-light renewable NIR persistent luminescence,[26] is used as the PLNP to achieve autofluorescence-free bioimaging. Furthermore, TPP with high lipophilicity serves as the targeting moiety to facilitate the transportation of the nanoprobe across the mitochondrial membrane owing to its special property of delocalized positive charge.[27,28] The PLNP is coated with (3-aminopropyl)triethoxysilane (APTES) to prepare amino-functionalized PLNP (PLNP-$NH_2$). Further conjugation of TPP to PLNP-$NH_2$ through carbodiimide reaction gives PLNP-TPP. The prepared PLNP-TPP is capable to transport across mitochondrial membrane for autofluorescence-free targeted imaging of mitochondria in cancer cells.

## 2. Results and Discussion

### 2.1. Preparation, Characterization and Optical Properties of PLNP-TPP

**Scheme 1** illustrates the preparation and application of PLNP-TPP for mitochondria targeted imaging. The NIR-emitting PLNP was hydrothermally synthesized with the feeding molar ratio of 1.6:1.6:0.2:0.005 for Zn:Ga:Ge:Cr at 220 ℃ for 10 h to obtain the optimal persistent luminescence and afterglow time (Figure S1-S3, Supporting Information**).** The as-synthesized PLNP is spherical **(Figure 1**A**)** with an average size of 17 nm (calculated from 100 randomly selected particles (Figure S4, Supporting Information) and the spinel phase of $ZnGa_2O_4$ and

$Zn_2GeO_4$ with the diffraction peaks at 18.3°, 30.2°, 35.4°, 37.1°, 43.1°, 53.4°, 56.9° and 62.5° (Figure 1B).

The hydroxylation of the PLNP gave more negatively charged PLNP-OH (**Figure 2**A). Further coating of APTES offered positively charged nanoparticles with the broad peak at 3480 $cm^{-1}$ - 3052 $cm^{-1}$ and a peak around 1560 $cm^{-1}$ for $–NH_2$ in the FT-IR spectra (Figure 2A and 2B),[29] confirming the successful preparation of PLNP-$NH_2$. Subsequent carbodiimide reaction between TPP and PLNP-$NH_2$ led to an increase in hydrodynamic size of the nanoparticles from 40.8 to 64.5 nm with the disappearance of the characteristic peak at 1560 $cm^{-1}$ for N-H stretching vibration and the increase of the peak at 1450 $cm^{-1}$for C-N stretching vibration in the FT-IR spectra (Figure 2B and 2C),[30] and the appearance of new absorption peaks at 224 nm and 267 nm for TPP in the UV-vis spectra (Figure 2D), indicating the successful conjugation of TPP on the surface of PLNP-$NH_2$. The PLNP-TPP showed similar average size (18 nm) and XRD pattern to PLNP (Figure S5, Supporting Information), suggesting no significant effect of amino-functionalization and TPP conjugation on the crystal structure and morphology of PLNP.

PLNP-$NH_2$ had a slight weight loss below 120 ℃ but an obvious weight loss in the temperature range of 300-550 ℃, indicating the pyrolysis of APTES.[24] PLNP-TPP lost more weight than PLNP-$NH_2$ as temperature increased due to the further loss of organic moiety TPP (Figure 2E). The weight percentages of the organic moieties on PLNP-$NH_2$ and PLNP-TPP were estimated to be 1.5% and 3.6%, respectively. PLNP-TPP showed good photostability and dispersibility in water while its colloidal solution was stable at least for 30 min (Figure 2F; Figure S6, Supporting Information).

The as-prepared PLNP gave an NIR emission at 695 nm due to the $^2E \rightarrow {}^4A_2$ transition of $Cr^{3+}$ ions in gallogermanate **(Figure 3**A, red line**)**,[31] and a broad excitation range **(**Figure 3A, black line**)** with the strong band at 254 nm as a result of the combination of the ZGGO host

excitation and the O−Cr charge transfer, the band at 296 nm for band-to-band excitation and other bands at 380-420 nm ($^4A_2 \rightarrow {}^4T_1$ transitions) and 520-600 nm ($^4A_2 \rightarrow {}^4T_2$ transitions) from the $Cr^{3+}$ d-d transitions in the luminescence center.[28,32,33] Additionally, the as-prepared PLNP had intense long-lasting phosphorescence (LLP) at 695 nm after 10 min UV excitation **(**Figure 3B**)**.

The luminescence of the as-synthesized PLNP can be activated with a visible light whether UV pre-irradiation was applied or not (Figure S7, Supporting Information). No significant shift of the emission spectrum of PLNP was observed under the excitation in the range of 520-600 nm (Figure S8, Supporting Information**)**. The LLP of the PLNP had no significant change during five replicate 560-nm excitations (Figure S9, Supporting Information). In addition, the persistent luminescence was still detectible on a CCD camera for 24 h after removal of 254-nm UV lamp (Figure 3C). Furthermore, the PLNP and PLNP-TPP can be activated and re-activated with Xe lamp irradiation without UV pre-irradiation **(**Figure 3D; Figure S10, Supporting Information**)**. The above results show that the as-synthesized PLNP or PLNP-TPP can be activated with visible light for bioimaging which is no longer limited by the afterglow time.

**2.2. Cytotoxicity Assay and Cellular Uptake of PLNP-TPP.**

To evaluate the potential cytotoxicity of PLNP-TPP, the viability of 3T3, HepG2 and HeLa cells after incubation with various concentrations (0-300 μg $mL^{-1}$) of PLNP-TPP for 48 h was measured via the standard MTT assay (**Figure 4**A). No significant reduction of the viability of the studied lines of cells was observed in the presence of PLNP-TPP from 50 to 300 μg $mL^{-1}$, indicating the negligible cytotoxicity of PLNP-TPP.

To further investigate the cell uptake performance of PLNP-TPP, 3T3, HepG2 and HeLa cells were used as model cells to incubate with PLNP-TPP (150 μg $mL^{-1}$) for 48 h while the cells treated with the PLNP were taken as control. These cells were then fixed with

paraformaldehyde and finally imaged on CLSM. The relative fluorescence intensity and the CLSM images of 3T3, HepG2 and HeLa were shown in Figure 4B and 4C, respectively. For the cells incubated with PLNP-TPP, the internalization of PLNP-TPP was clearly observed in both cancer (HepG2 and HeLa) and normal (3T3) cells and the fluorescence intensity of HepG2 and HeLa cells was about 4.3 and 3.8 folds higher than 3T3 cells, respectively. However, for the cells incubated with PLNP, the fluorescence intensity of HepG2 and HeLa cells changed slightly due to the poor dispersibility of PLNP. These results suggest that the PLNP-TPP can directly infiltrate into the cells by endocytosis and more easily internalized by both HepG2 and HeLa cells.

**2.3. PLNP-TPP for Selective Mitochondrial Targeting in Cancer Cells**

Co-localization imaging in HepG2 cells was performed on CLSM to show whether the PLNP-TPP could selectively locate in mitochondria. Mito-tracker Green, a commercial mitochondrial-specific dye, was chosen to stain mitochondria.[34-36] The PLNP or PLNP-TPP incubated HepG2 cells were stained with Mito-Tracker Green to label mitochondria. **Figure 5** shows the CLSM images for the cells co-stained by the Mito-Tracker Green (green signal) and the nanoparticle (red signal). The merged images show greater overlap for the Mito-Tracker Green/PLNP-TPP pair than Mito-Tracker Green/PLNP pair (as evidenced by the clear yellow signals). The above observation was further confirmed by quantifying the line scanning profiles of luminescence intensity and the colocalization ratio of the merged images of HepG2 cells was 47.7% for PLNP and 47.5% for PLNP-TPP. In addition, the Pearson's coefficient of the merged images of HepG2 cells was 0.216 for PLNP and 0.584 for PLNP-TPP. The same is also true for another cancer cell line, HeLa cell (Figure S11, Supporting Information) and the colocalization ratio of the merged images of HeLa cells was 59.7% and the Pearson's coefficient of the merged images of HeLa cells was 0.611. These results suggest that the PLNP-TPP has the ability to transport across mitochondrial membrane and get to the

mitochondria of cancer cells owing to the high negatively charge of the mitochondrial membrane.[37]

To show whether the PLNP-TPP can specifically stain the mitochondrial region in live cancer cells, co-localization imaging experiments were also performed on 3T3 cells for comparison. As shown in Figure 5, the co-localization images of 3T3 cells as well as the quantification of the line scanning profiles of luminescence show poor overlap for both the Mito-Tracker Green/PLNP pair and Mito-Tracker Green/PLNP-TPP pair and the colocalization ratio was 53.6% for PLNP and 44.4% for PLNP-TPP. Similarly, the Pearson's coefficient of the merged images of 3T3 cells was 0.136 and for PLNP and 0.158 for PLNP-TPP and no obvious co-coloration could be found in the merged image of 3T3. All the above results indicate that PLNP-TPP enables specific staining of the mitochondrial region in live cancer cells with the TPP targeting ligand due to higher mitochondrial membrane potential in cancer cells.[37,38]

**2.4. Persistent Luminescence (PL) Imaging in vivo**

To further investigate whether the PLNP-TPP can eliminate tissue autofluorescence, 200 μL of 1 mg $mL^{-1}$ PLNP-TPP was administered to tumor-bearing BALB/c nude mice and normal BALB/c nude mice via orthotopic injection after 10-min pre-irradiated with Xe lamp. As shown in **Figure 6**A, the normal BALB/c nude mice treated with PLNP-TPP displayed a strong luminescence signal without tissue autofluorescence and the same is also true for tumor-bearing BALB/c nude mice (Figure 6B). However, in the control group (Figure 6C), the fluorescence signal of the mice treated with Mito-tracker Green (200 μL, 200 nM) was rather weak owing to the high tissue autofluorescence, indicating that PLNPs-TPP had the potential ability to act as an autofluorescence-free mitochondria targeting nanoprobe without excitation in vivo for in vivo applications.

**3. Conclusion**

In conclusion, we have developed a visible light activatable TPP functionalized NIR persistent luminescence nanoprobe PLNP-TPP for mitochondria-targeted imaging in cancer cells. The developed PLNP-TPP nanoplatform has several advantages for bioimaging. In comparison with traditional organic dyes, the PLNP-TPP effectively avoids tissue autofluorescence interference due to its long afterglow nature. It also has excellent properties in biological imaging, including photostability, dispersibility and biocompatibility. Furthermore, the PLNP-TPP has the ability to transport across mitochondrial membrane and specifically accumulate in the mitochondria of cancer cells, showing great potential for autofluorescence-free targeting bioimaging of mitochondria in cancer cells.

## 4. Experimental Section

*Synthesis of PLNP:* The PLNP ($Zn_{1.6}Ga_{1.6}Ge_{0.2}O_4$:Cr(III)) was synthesized via a hydrothermal method according to previous publications with minor modification.[22,27] Briefly, the predetermined molar ratio of Zn(II), Ga(III), Ge(IV), and Cr(III) precursor solutions were mixed under vigorous stirring. Then, ammonia hydroxide solution (28% , wt) was used to adjust pH to 9.0-9.5. After stirring for 1.5 h, the mixture solution was transferred to a Teflon-lined autoclave (50 mL) for 10- h hydrothermal reaction at 220 °C, then cooled naturally to room temperature. The resulting white precipitate PLNP was collected by centrifugation, re-dispersed in 0.01 M HCl, and sonicated for 30 min to remove ZnO impurity. The obtained PLNP was washed with excess isopropanol, collected by centrifugation, and freeze-dried for further use.

*Surface Functionalization of PLNP:* The hydroxylation and amino-functionalization of PLNP were conducted according to a previous work with slight modification.[19] Briefly, the PLNP powder was dispersed in 5 mM NaOH solution under sonication for 1 h, then vigorously stirred for 24 h. The hydroxylated PLNP (PLNP-OH) was collected by centrifuged at 10000 rpm for 15 min and washed with water three times. Finally, the PLNP-OH powder was obtained by freeze-drying for further use.

To prepare PLNP-$NH_2$, 50 mg of PLNP-OH was re-dispersed in 20 mL of dimethylformamide (DMF) under sonication, then 200 μL of APTES was added under vigorous stirring at 80 °C for 24 h. The resulting PLNP-$NH_2$ was collected by centrifugation, and washed with DMF to remove unreacted APTES.

To prepare PLNP-TPP, 50 mg of TPP was dispersed in 10 mL water, then *N*-(3-dimethylaminopropyl)-*N*′-ethylcarbodiimide hydrochloride (EDC) (25 mg) and *N*-hydroxysuccinimide (NHS) (35 mg) were added. The mixture was gently stirred at room temperature for 2 h. 10 mL of PLNP-$NH_2$ (1 mg $mL^{-1}$) was then added, and the mixture solution was stirred in dark at room temperature for 48 h. The unreacted TPP was removed by centrifugation and the resulting PLNP-TPP was washed with water three times and freeze-dried for further use.

*Cells and Cell Culture.* Two cancer cell lines, HepG2 (a human hepatoma cell line) and HeLa cells (a human cervical adenocarcinoma cell line) as well as a normal cell line 3T3 were cultured in Dulbecco's modified Eagle's high-glucose medium (DMEM) supplemented with 10% fetal bovine serum (FBS) and 1% penicillin−streptomycin solution at 37 °C in 5% $CO_2$.

*Cell Viability Assay:* A standard MTT assay was applied to measure the viability of HeLa, HepG2 and 3T3 cells. Briefly, the cells (ca. $10^4$ per well) were seeded in 96-well plates and cultured in DMEM medium supplemented with 10% FBS and and 1% penicillin−streptomycin solution in 5% $CO_2$ at 37 °C. After 24-h incubation, the cells were washed with PBS buffer. Then, the fresh medium containing PLNP-TPP with desired concentrations (0, 0.05, 0.1, 0.15, 0.2, 0.25, and 0.3 mg $mL^{-1}$) was added into 96-well plates and the resultant cell mixture was subject to 48-h incubation. Afterwards, the wells were washed with PBS buffer and incubated with DMEM containing 0.5 mg $mL^{-1}$ MTT for another 4 h. After removing the culture medium, 150 μL of dimethylsulfoxide (DMSO) was added to dissolve the precipitates and the absorbance at 570 nm was measured on a BioTek Synergy H1 microplate reader to calculate the viability.

*Cells Uptake of PLNP-TPP:* The uptake of PLNP-TPP on 3T3, HeLa and HepG2 cells was observed on a laser confocal scanning microscope (CLSM). Briefly, the cells were seeded on cover slides in a 6-well culture plate and incubated 24 h to obtain monolayer cells. Subsequently, 1 mL of the fresh medium containing PLNP-TPP (0.15 mg $mL^{-1}$) was added to the wells and incubated for 48 h. Then, the cells were washed with PBS three times and 1 mL of paraformaldehyde (4%) was then used to fix the cells for 10 min. Finally, Olympus Fluoview FV3000 instrument was used to record the fluorescent images of the cells. The fluorescence of PLNP-TPP was excited at 561 nm. All fluorescence channels were detected sequentially.

*Selective Mitochondrial Targeting of PLNP-TPP:* Briefly, the HepG2 cells or 3T3 cells were seeded on cover slides in a 6-well culture plate and incubated 24 h to obtain monolayer cells. Then, the cells were washed with PBS three times. Subsequently, 1 mL of the fresh medium containing PLNP-TPP (0.15 mg $mL^{-1}$) or PLNP (0.15 mg $mL^{-1}$) was added to the wells and incubated for 48 h. After washing with PBS for three times, 1 mL of the fresh medium containing Mito-tracker Green (200 nM) was added to the wells and incubated for 20 min, then 1 mL of paraformaldehyde (4%) was used to fix the cells for 10 min. Finally, Olympus Fluoview FV3000 instrument was used to record the fluorescent images of the cells. The fluorescence of PLNP-TPP and Mito-tracker Green was excited at 561 nm and 488 nm, respectively. All fluorescence channels were detected sequentially.

*Co-localization Imaging of HeLa and HepG2 Cells:* Briefly, the HepG2 and HeLa cells were seeded on cover slides in a 6-well culture plate and incubated for 24 h to obtain monolayer cells. Then, the cells were washed with PBS three times. Subsequently, 1 mL of the fresh medium containing PLNP-TPP (0.15 mg $mL^{-1}$) was added to the wells and incubated for 48 h. After washing with PBS for three times, 1 mL of the fresh medium containing Mito-tracker Green (200 nM) was added to the wells and incubated for 20 min, then 1 mL of paraformaldehyde (4%) was used to fix the cells for 10 min. Finally, Olympus Fluoview

FV3000 instrument was used to record the fluorescent images of the cells. The fluorescence of PLNP-TPP and Mito-tracker Green was excited at 561 nm and 488 nm, respectively. All fluorescence channels were detected sequentially.

*In vivo Persistent Luminescence Imaging:* BALB/c nude mice were obtained from Shanghai Slac Laboratory Animal Co. Ltd (Shanghai, China). All animal experimental protocols were in accordance with the guidelines of the regional ethic committee and approved by the Animal Ethics Committee of Jiangnan University.

The nude mice were anesthetized with 4% chloral hydrate via intraperitoneal administration. PLNP-TPP (200 μL, 1 mg $mL^{-1}$ in PBS at pH 7.4) was administered to nude mice via orthotopic injection after 10-min pre-irradiated with Xe lamp, and in vivo bioimaging was carried out without in situ excitation (exposure time: 60 s). For comparison, Mito-tracker Green (200 μL, 200 nM in PBS at pH 7.4) was administered to nude mice via orthotopic injection and the signals were collected at ex=480 nm and em=570 nm.

**Supporting Information**
Supporting Information is available from the Wiley Online Library or from the author.

**Acknowledgements**
The authors appreciate the financial support from the National Natural Science Foundation of China (No. 21934002, 21804056 and 21804057), the China Postdoctoral Science Foundation (No. 2018M630511 and 2018M630509), the Postdoctoral Innovative Talent Support Program (No. BX20180130), and the Natural Science Foundation of Jiangsu Province, China (No. BK20180581 and BK20180584), the National First-class Discipline Program of Food Science and Technology (No. JUFSTR20180301), the Fundamental Research Funds for the Central Universities (No. JUSRP51714B and JUSRP11846), and Collaborative Innovation Center of Food Safety and Quality Control in Jiangsu Province.

**Conflict of Interest**
The authors declare no conflict of interest.

Received: ((will be filled in by the editorial staff))
Revised: ((will be filled in by the editorial staff))
Published online: ((will be filled in by the editorial staff))

**References**

[1] M. Saraste, *Science* **1999**, *283*, 1488.

[2] V. Gogvadze, S. Orrenius, B. Zhivotovsky, *Semin. Cancer Biol.*, **2009**, *19*, 57.

[3] X. Ma, N. Gong, L. Zhong, J. Sun, X.-J. Liang, *Biomaterials*, **2016**, *97*, 10.

[4] Y. Shen, L. Liang, S. Zhang, D. Huang, R. Deng, J. Zhang, H. Qu, S. Xu, C. Liang and W. Xu, *ACS Appl. Mater. Interfaces*, **2018**, *10*, 7910.

[5] G. Kroemer, J. C. Reed, *Nat. Med.*, **2000**, *6*, 513.

[6] Q. Qu, X. Ma and Y. Zhao, *Nanoscale*, **2015**, *7*, 16677.

[7] G. Kroemer, J. Pouyssegur, *Cancer Cell*, **2008**, *13*, 472.

[8] P. Yuan, X. Mao, X. Wu, S. S. Liew, L. Li and S. Q. Yao, *Angew. Chem. Int. Ed.*, **2019**, *58*, 1.

[9] V. Gogvadze, *Curr. Pharm. Des.*, **2011**, *17*, 4034.

[10] N. Zhao, S. Chen, Y. Hong and B. Z. Tang, *Chem. Commun.*, **2015**, *51*, 13599.

[11] Y. C. Wong, D. Ysselstein, D. Krainc, *Nature*, **2018**, *554*, 382.

[12] Z. Liu, H. Pei, L.Zhang and Y. Tian, *ACS Nano*, **2018**, *12*, 12357.

[13] H. Huang, F. Dong, and Y. Tian, *Anal. Chem.*, **2016**, *88*, 12294.

[14] X. Hu, Y. Li, T. Liu, G. Zhang, and S. Liu, *ACS Appl. Mater. Interfaces*, **2015**, *7*, 15551.

[15] X. Liu, M. Li, T. Han, B. Cao, Z. Qiu, Y. Li, Q. Li, Y. Hu, Z. Liu, J. W. Y. Lam, X. Hu, and B. Z. Tang, *J. Am. Chem. Soc.*, **2019**, *141*, 11259.

[16] W. Zhang, X. Hu, Q. Shen, and Da Xing, *Nat. Commun.*, **2019**, *10*, 1704.

[17] D. Zhang, L. Wen, R. Huang, H. Wang, X. Hu, D. Xing, *Biomaterials*, **2018**, *153*, 14.

[18] H. Yamamoto, T. Matsuzawa, *J. Lumin.*, **1997**, *72*, 287.

[19] Z. Pan, Y.-Y. Lu and F. Liu, *Nature materials*, **2012**, *11*, 58.

[20] T. Matsuzawa, Y. Aoki, N. Takeuchi and Y. Murayama, *J. Electrochem. Soc.*, 1996, *143*, 2670.

[21] S.-K. Sun, H-F Wang and X-P Yan, *Acc. Chem. Res.* 2018, *51*, 1131.

[22] X. Zhao, L. -J. Chen, K. -C. Zhao, Y.-S. Liu, J.-L. Liu and X. -P. Yan, *Trends Anal. Chem.*, 2019, *118*, 65.

[23] T. Maldiney, A. Lecointre, B. Viana, A. Bessière, M. Bessodes, D. Gourier, C. Richard and D. Scherman, *J. Am. Chem. Soc.*, **2011**, *133*, 11810.

[24] A. Abdukayum, J.-T. Chen, Q. Zhao and X.-P. Yan, *J. Am. Chem. Soc.*, **2013**, *135*, 14125.

[25] Y.-J. Li and X.-P. Yan, *Nanoscale*, **2016**, *8*, 14965.

[26] Z. Li, Y. Zhang, X. Wu, L. Huang, D. Li, W. Fan and G. Han, *J. Am. Chem. Soc*., **2015**, *137*, 5304.

[27] Y. Zhang, C. Zhang, J. Chen, L. Liu, M. Hu, J. Li and H. Bi, *ACS Appl. Mater. Interfaces*, **2017**, *9*, 25152.

[28] R. A. J. Smith, C. M. Porteous, A. M. Gane and M. P. Murphy, *Proc. Natl. Acad. Sci. U. S. A.*, **2003**, *100*, 5407.

[29] L. Zhang, J. Lei, J. Liu, F. Ma and H. Ju, *Biomaterials*, **2015**, *67*, 323.

[30] H. -X. Zhao, C. -X. Yang and X.-P. Yan, *Nanoscale*, **2016**, *8*, 18987.

[31] J. Wang, Q. Ma, X.-X. Hu, H. Liu, W. Zheng, X. Chen, Q. Yuan and W. Tan, *ACS Nano* **2017**, *11*, 8010.

[32] T. Maldiney, A. Bessière, J. Seguin, E. Teston, S. K. Sharma, B. Viana, A. J. J. Bos, P. Dorenbos, M. Bessodes, D. Gourier, D. Scherman and C. Richard, *Nature materials*, **2014**, *13*, 418.

[33] A. BessiŁre, S. K. Sharma, N. Basavaraju, K. R. Priolkar, L. Binet, B. Viana, A. J. J. Bos, T. Maldiney, C. Richard, D. Scherma and D. Gourier, *Chem. Mater.*, **2014**, *26*, 1365.

[34] Y. Sun, Y. Chen, X. Ma, Y. Yuan, C. Liu, J. Kohn and J. Qian, *ACS Appl. Mater. Interfaces*, **2016**, *8*, 25680.

[35] R. Guo , H. Peng , Y. Tian , S. Shen and W. Yang, *Small*, **2016**, *12*, 4541.

[36] Y. Guan, H. Lu, W. Li, Y. Zheng, Z. Jiang, J. Zou and H. Gao, *ACS Appl. Mater. Interfaces*, **2017**, *9*, 26731.

[37] J. S. Modica-Napolitano and V. Weissig, *Int. J. Mol. Sci.*, **2015**, *16*, 17394.

[38] Y. Zhang, C. Zhang, J. Chen, L. Liu, M. Hu, J. Li and H. Bi. *ACS Appl. Mater. Interfaces*, **2017**, *9*, 25152

10.1002/cnma.201900697

WILEY-VCH

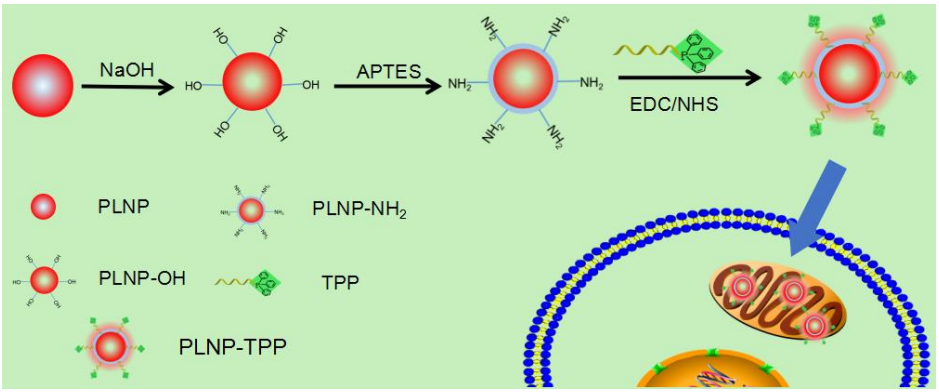


**Scheme 1.** Illustration of the preparation of the functional persistent luminescence nanoprobe PLNP-TPP for mitochondria targeted imaging.

10.1002/cnma.201900697

WILEY-VCH

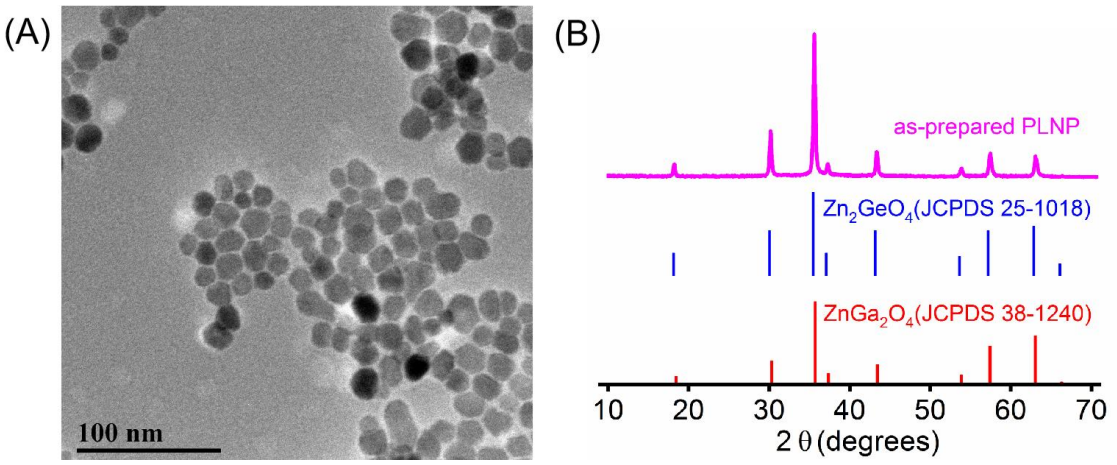


**Figure 1.** (A) TEM image of the as-prepared PLNP. (B) XRD pattern of the as-prepared PLNP.

10.1002/cnma.201900697

WILEY-VCH

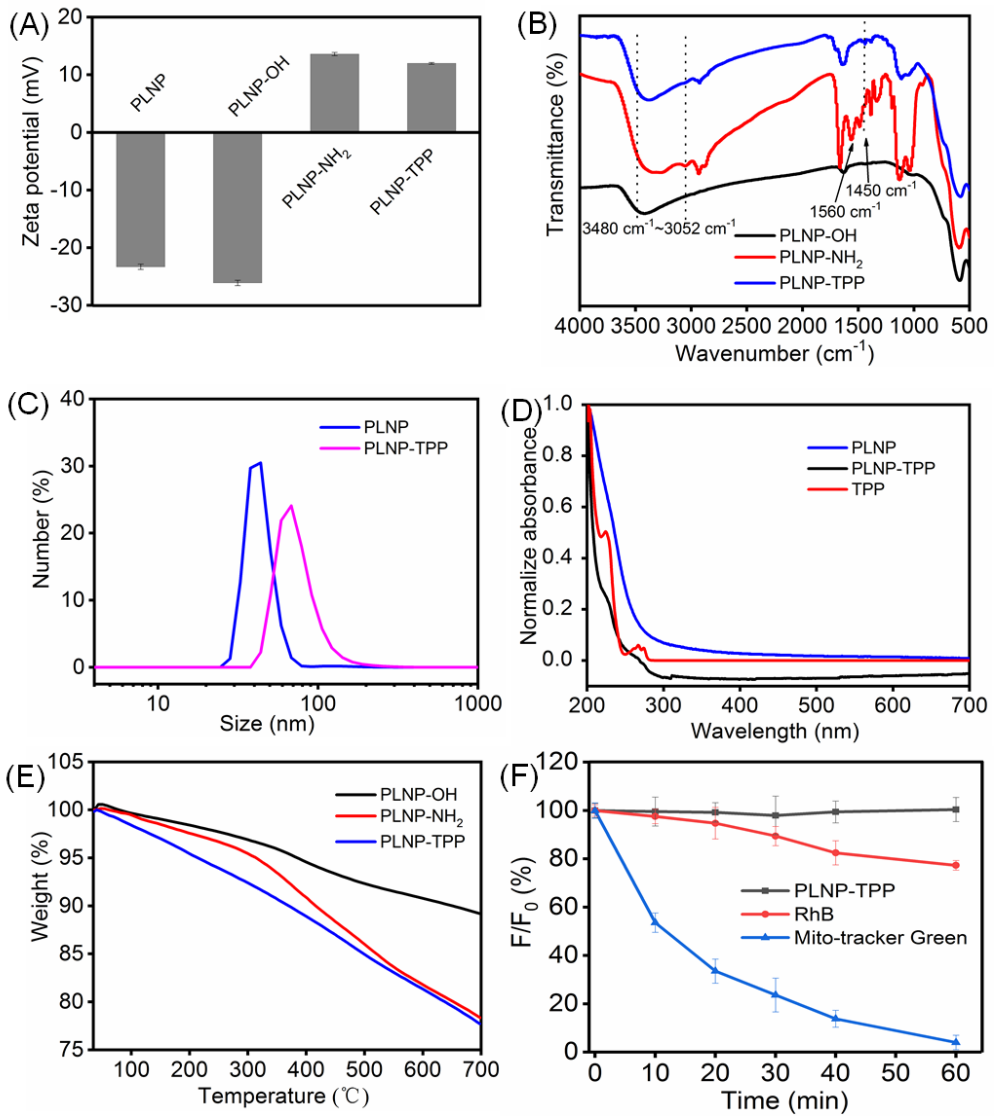


Figure 2. (A) Zeta potentials of PLNP, PLNP-OH, PLNP-$NH_2$ and PLNP-TPP in PB solution (1 mM, pH 7.5). (B) FT-IR spectra of PLNP-OH, PLNP-$NH_2$, PLNP-TPP. (C) Hydrodynamic size distribution of PLNP and PLNP-TPP in water. (D) UV-Vis spectra of PLNP, PLNP-TPP and TPP. (E) TGA curves of PLNP-OH, PLNP-$NH_2$, and PLNP-TPP. (F) Photostability of PLNP-TPP, RhB and Mito-tracker Green under UV lamp irradiation. $F_0$ and F are the luminescence intensity without UV lamp irradiation and with UV lamp irradiation at a certain time, respectively.

10.1002/cnma.201900697

WILEY-VCH

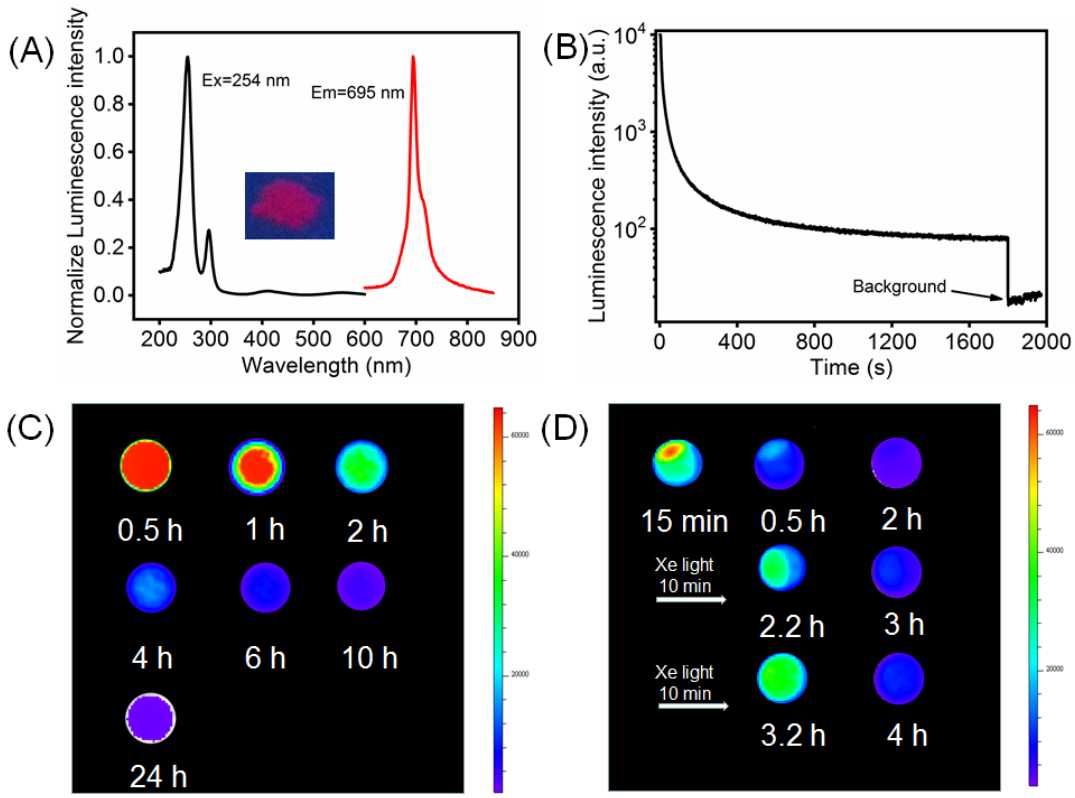


**Figure 3.** (A) Excitation (black curve, em. 695 nm) and emission (red curve, ex. 254 nm) spectra of the as-prepared PLNP powder. The inset shows the digital photo of PLNP powder under 254-nm UV lamp irradiation. (B) Persistent luminescence decay curve for the as-prepared PLNP powder, monitored at 695 nm after 254-nm UV lamp irradiation for 10 min. (C) NIR persistent luminescence images after 254-nm UV lamp irradiation (6W) for 10 min. (D) Visible light-reactivated persistent luminescence images of the PLNP powder after 10-min Xe lamp irradiation (6W) without 254 nm pre-irradiation.

10.1002/cnma.201900697

WILEY-VCH

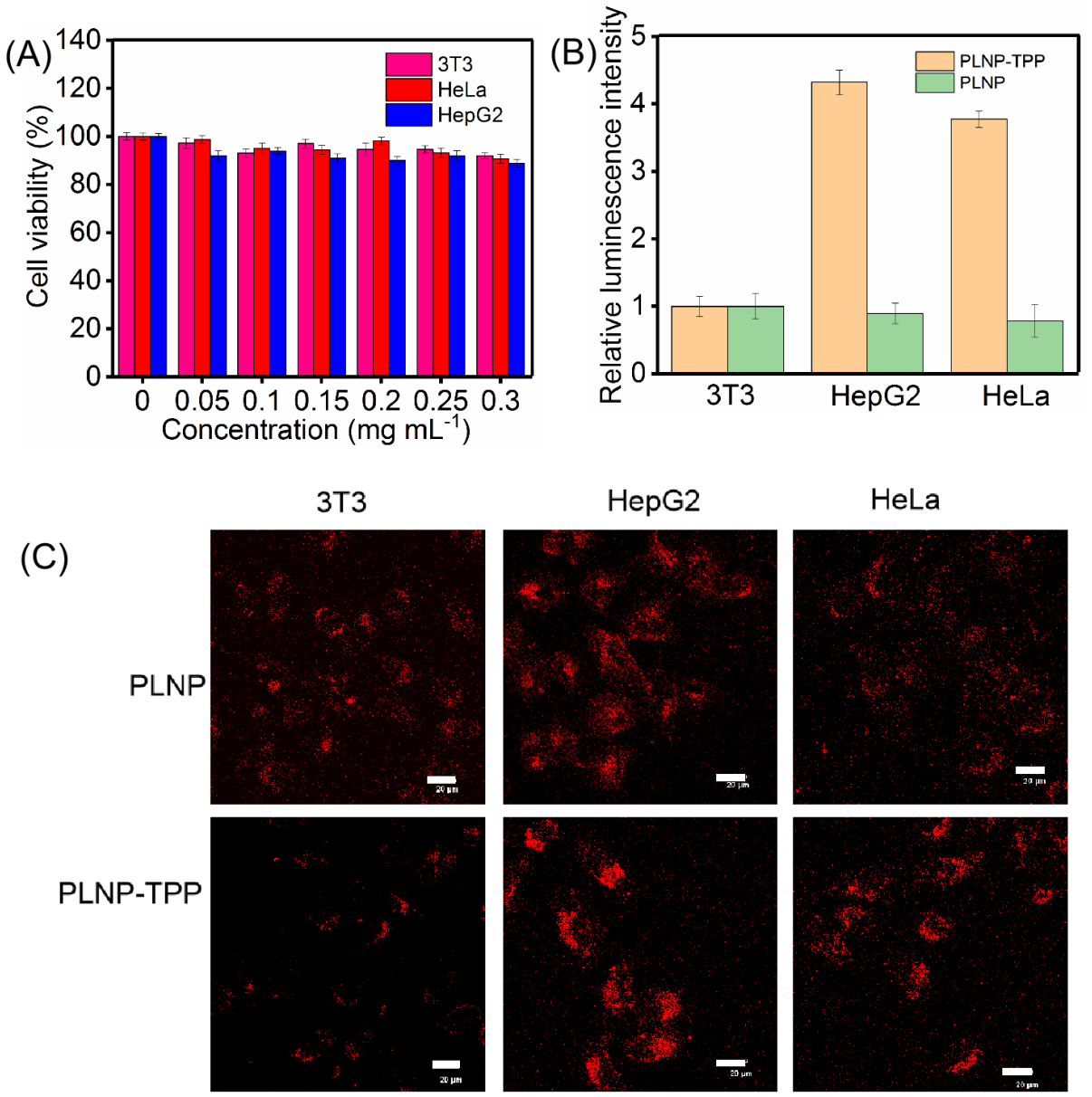


**Figure 4.** (A) Viability of 3T3, HepG2 and HeLa cells treated with various concentrations of PLNP-TPP. (B) Relative luminescence intensity of 3T3, HepG2 and HeLa cells treated with PLNP and PLNP-TPP (the fluorescence intensity of 3T3 was taken as 1). (C) CLSM images of 3T3, HepG2 and HeLa cells after incubation with PLNP and PLNP-TPP (0.15 mg $mL^{-1}$) for 48 h. Red channel was excited at 561 nm. Scale bars are 20 μm.

10.1002/cnma.201900697

WILEY-VCH

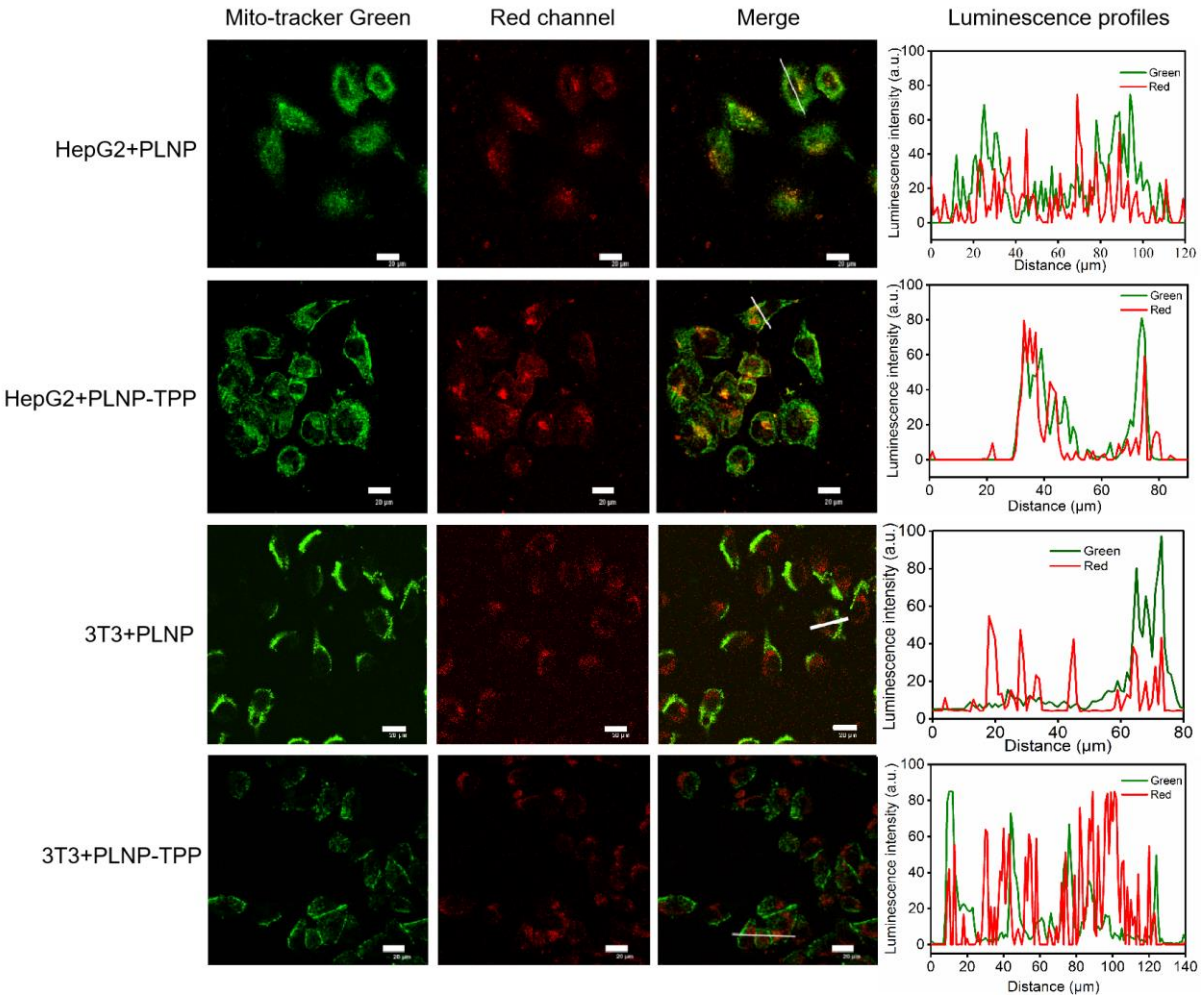


**Figure 5**. CLSM images of HepG2 cells and 3T3 cells treated with PLNP and PLNP-TPP. Luminescence profiles were obtained from the regions of interest (white line in merge images) across the lines. Green channels and red channels were excited at 488 and 561 nm, respectively. Scale bars are 20 μm.

10.1002/cnma.201900697

WILEY-VCH

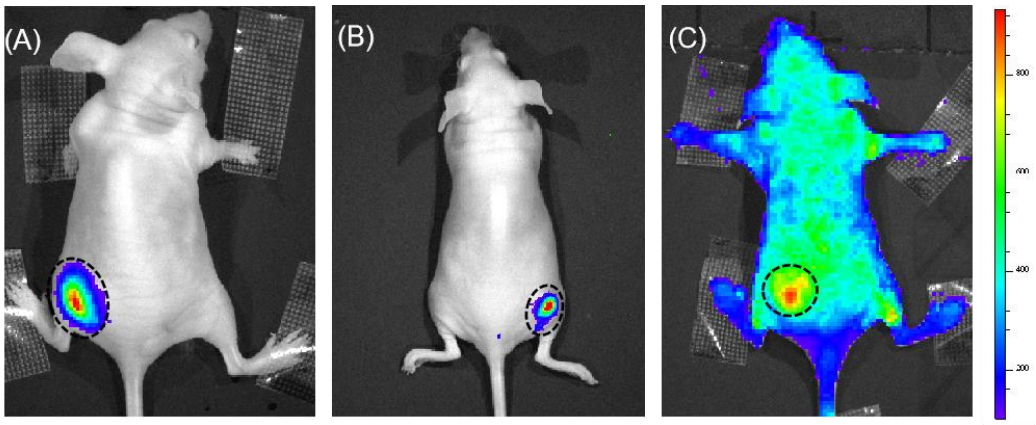


**Figure 6**. In vivo near-infrared persistent luminescence images of normal mice (A) and tumor-bearing mice (B) after orthotopic injection of PLNP-TPP (irradiated with visible light for 10 min before injection). (C) In vivo mice imaging after orthotopic injection of Mito-tracker Green (ex=480 nm, em= 570 nm).

10.1002/cnma.201900697

WILEY-VCH

**The table of contents entry**
TPP functionalized NIR persistent luminescence nanoprobe was developed for mitochondria-targeted imaging in cancer cells

**Keywords**
persistent luminescence; nanoprobe; mitochondria; cancer cells; bioimaging

*Yu-Bin Su, Xu Zhao, Li-Jian Chen, Hai-Long Qian, and Xiu-Ping Yan**

**Title**
6-triphenylphosphinehexanoic acid conjugated near-infrared persistent luminescence nanoprobe for autofluorescence-free targeted imaging of mitochondria in cancer cells